SCIENTIFIC REPORTS
nature research

OPEN

Genetic variation regulates opioid-induced respiratory depression in mice

Jason A. Bubier[1]✉, Hao He[1], Vivek M. Philip[1], Tyler Roy[1], Christian Monroy Hernandez[1], Rebecca Bernat[2], Kevin D. Donohue[2,3], Bruce F. O'Hara[2,4] & Elissa J. Chesler[1]

In the U.S., opioid prescription for treatment of pain nearly quadrupled from 1999 to 2014. The diversion and misuse of prescription opioids along with increased use of drugs like heroin and fentanyl, has led to an epidemic in addiction and overdose deaths. The most common cause of opioid overdose and death is opioid-induced respiratory depression (OIRD), a life-threatening depression in respiratory rate thought to be caused by stimulation of opioid receptors in the inspiratory-generating regions of the brain. Studies in mice have revealed that variation in opiate lethality is associated with strain differences, suggesting that sensitivity to OIRD is genetically determined. We first tested the hypothesis that genetic variation in inbred strains of mice influences the innate variability in opioid-induced responses in respiratory depression, recovery time and survival time. Using the founders of the advanced, high-diversity mouse population, the Diversity Outbred (DO), we found substantial sex and genetic effects on respiratory sensitivity and opiate lethality. We used DO mice treated with morphine to map quantitative trait loci for respiratory depression, recovery time and survival time. Trait mapping and integrative functional genomic analysis in GeneWeaver has allowed us to implicate *Galnt11*, an *N*-acetylgalactosaminyltransferase, as a gene that regulates OIRD.

An estimated 4 to 6% of patients who misuse prescription opioids switch to illicit drugs such as heroin[1,2] and about 80% of people who use heroin had first misused prescription opioids[1,2]. The non-uniform composition, dosing and administration of more potent synthetic street opioids including fentanyl frequently leads to overdose. Remedial measures such as treatment with naloxone, a competitive antagonist of the opioid receptor mu 1 (OPRM1), the principal target of opioids, are often unsuccessful due to the higher potency of synthetic opioids[3–5]. Therefore, novel approaches toward understanding opioid addiction, overdose and remediation are essential.

The most frequent cause of overdose death due to opioids is opioid-induced respiratory depression (OIRD). Opioids such as morphine depress the hypoxic ventilatory response in the brainstem by affecting the chemosensitive cells that respond to changes in the partial pressures of carbon dioxide and oxygen in the blood[6]. Understanding the underlying molecular mechanisms that control the respiratory responses to opioids may provide insight into alternative therapies for opioid overdose by treating the respiratory depression directly, independent of, or together with opioid receptor antagonism. Variable responses in OIRD have been well documented in both humans and mice[7], and likely occur through diversity in the molecular pathways within the ventilatory processing centers of the brainstem. Our goal is to utilize this genetic diversity to define genetic modifiers of OIRD in mice.

Genetic diversity in laboratory mice is a powerful tool for dissecting the genetic and molecular components of complex traits such as the response to opioids. In mice, genetic variation has been identified in the opioid receptors[8–12], in genes and pathways associated with the anti-nociceptive effects of morphine[13–18] and morphine withdrawal[19], and in other behavioral responses to opioids[17,20–24]. Other studies have characterized the median lethal dose (LD_{50}) of morphine across mouse strain[25]. One study found that a strain harboring an OPRM1 hypomorph (CXB7), in which OPRM1 gene function is reduced, have a much higher LD_{50} for morphine than strains with intact mu-opioid[8,24], confirming the importance of OPRM1 in opioid-induced lethality and revealing strain diversity in the mu-opioid receptor locus. Together, these studies show that variation in response to opioids is associated with differences in strain, indicating that responses to opioids are genetically influenced phenotypes. However, these studies were generally conducted on only a few strains of male mice with survival as the only

[1]The Jackson Laboratory, Bar Harbor, ME 04605, USA. [2]Signal Solutions, LLC, Lexington, KY, USA. [3]Electrical and Computer Engineering Department, University of Kentucky, Lexington, KY, USA. [4]Department of Biology, University of Kentucky, Lexington, KY, USA. ✉email: jason.bubier@jax.org

endpoint, and thus did not characterize known sex differences in opioid sensitivity[26] and were not designed to define the genetic loci or the underlying biological mechanisms responsible for the strain variation in complex opioid responses, such as respiratory depression.

Respiratory phenotyping in mice generally includes measures of ventilation mechanics such as respiratory frequency and tidal volume using conventional plethysmography. However, plethysmography is labor intensive and the duration over which the mouse can be monitored is limited because the animal is confined, and its movements are restricted. Further, monitoring the rapid response to drugs by plethysmography is invasive because it requires the surgical implantation of a cannula, catheter or other port into the mouse in order to administer the compounds. Here, we have taken the novel approach using signals obtained from a piezo electric sleep monitoring system[27] to measure respiratory phenotypes. This system offers a non-invasive, high-throughput technology to study respiratory depression in response to opioids in mice in a home-cage setting. The piezo technology was adapted to estimate average respiratory rates over specified time intervals for characterizing patterns associated with respiratory depression. This allows for the determination of respiratory depression and time to recovery or cessation of respiration. This system was previously validated and used by us in genetic studies of sleep in the Collaborative Cross (CC)[28,29], BXD [19], and other mouse populations[30].

In this study, we investigated the effect of genetic variation on OIRD and lethality in the founders of the advanced, high-diversity mouse populations, specifically the CC and Diversity Outbred (DO) populations. After determining that the quantitative respiratory phenotypes were heritable and that genetic mapping was therefore feasible, we mapped key respiratory traits using a population of 300 DO mice of both sexes and our advanced piezo electric sleep monitoring system[27]. This enabled us to reveal a previously undiscovered potential mechanism of variability in OIRD, which was further evaluated through analysis of sequence variation, gene expression and conservation of protein domains.

Results

Development of a high-throughput method for measuring respiratory depression in response to opioids. The PiezoSleep system measures pressure on the mouse cage floor to determine sleep or wake behaviors over small time interval. In addition to responding to pressure from gross body movements, the sensors also respond to thorax motion. The current commercial system provides estimates of respiration rates during detected sleep states; however, for this study a custom algorithm was developed to estimate respiration rates on low activity segment during wake. Figure 1 illustrates the piezoelectric sensor capability by comparing simultaneous recordings from the plesthysmography and piezoelectric sensors. Very good signal agreement is observed between the plethysmography and piezoelectric signals during periods of low activity. Figure 1A compares signals when the mouse is likely resting (no body motion). The only motion from the mouse is from the thorax due to breathing, creating pressure on the cage floor that follows the changing air flow/pressure, as tracked by the plethysmography signal. Figure 1B compare signals when there is some form of low to moderate motion, such as slow locomotion or head movements. Amplitudes represent pressure but are normalized in the figure for comparing their dynamics. Amplitude changes for the piezoelectric signals depend on posture and contact with the cage floor, while the plethysmography signals directly measure the changes air pressure from breathing. The other body movements result in greater amplitude variation in the piezo signals; however, the breathing patterns from the plethysmography signals are still observable riding on top of these larger amplitude swings (Fig. 1B). Very high activity levels result in obscuring the breathing signal, eventually to a point that it cannot be estimated reliably.

The algorithm developed for this work extracts breath rates with short-time autocorrelation functions (4 s) to suppress aperiodic signal components from body motions.[27] This approach is particularly effective on signals like those shown in Fig. 1B. Estimates are only made when signal energy is below a threshold, where body motion does not obscure the thorax pressure changes. To assess the limitations of extracting breath rates this way, the algorithm was applied to 19 simultaneous recordings (about 19 total hours of data) on mice with the plethysmography and piezoelectric sensors. Results from comparing estimates from 4 s intervals over the whole data set, show a 3% underestimation for the piezoelectric method. This combines low activity (resting/sleeping) and moderate activity intervals. For just the low activity intervals (a little less than half the data) there was a slight over estimation of 0.2% (effectively zero, which is consistent with what is expected from the agreement shown Fig. 1). For the moderate activity intervals there was an underestimation of 6%. For this study it is likely that the baseline estimate for computing respiratory depression was similar in composition to the total data set, and a 3% negative bias is expected. In the high activity period after the injections, the bias value is expected to approach the 6% limit. Therefore, it is expected that a 3% increase in the respiratory depression estimate can result from the higher number of activity intervals during the opioid response.

For the application of the algorithm to this study, estimates were performed in the low to moderate activity regions and these values were averaged over much larger intervals to provide an average respiration rate every 12 min. This was used to obtain a baseline rate (averaged over a full 24 h pretreatment) and a stable estimate of percent respiratory depression post-treatment every 12 min. This interval was large enough so that even in high activity regions there were typically 30 or more intervals where estimates could be made and averaged together. The resulting derived measures enabled a quantitative evaluation of respiratory depression, survival time and recovery time (Fig. 2).

Respiratory depression, recovery time and survival time are largely uncorrelated and heritable traits. A bracketing approach was used to construct a dose–response curve with a minimal number of mice. Eight inbred strains of mice (CC and DO founders) of both sexes were tested with an initial probe dose of 436 mg/kg of morphine. We found a wide range of outcomes for respiratory depression (49% to 77%),

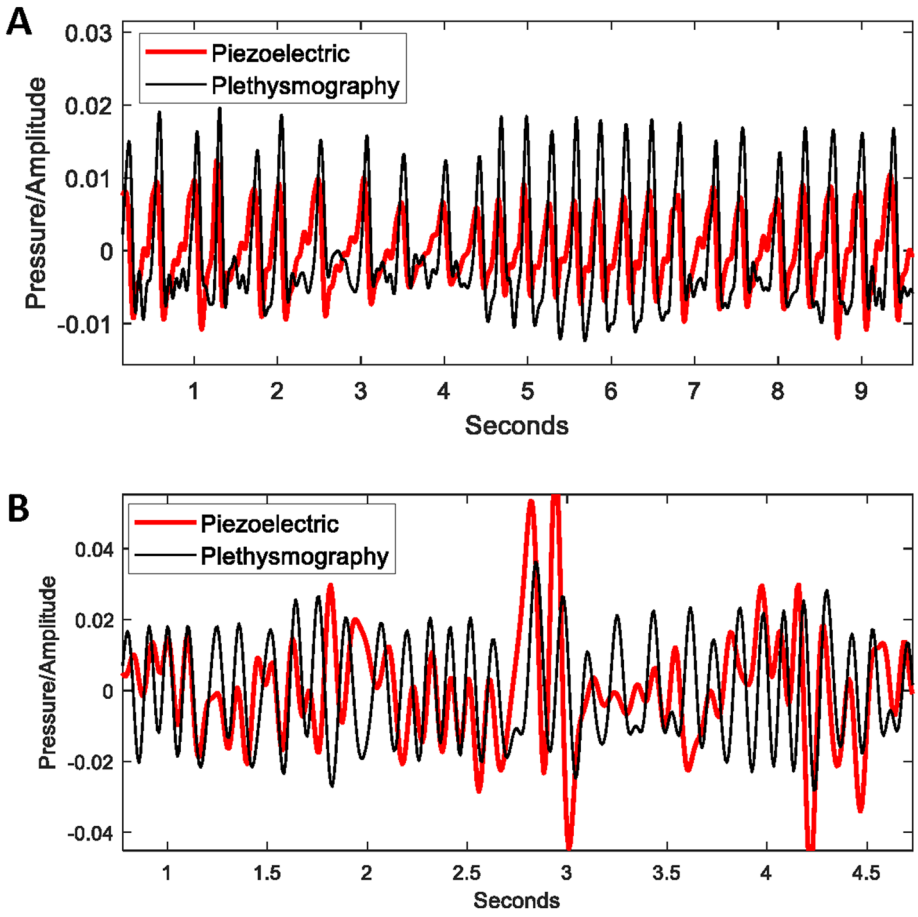

Figure 1. Simultaneous piezoelectric floor sensor and plethysmography signals are compared for extracting mean respiration rates over short-time intervals. (**A**) Example of low activity, sleep-like segment with piezoelectric signal generated from thorax motion with a strict correspondence to the changing air pressure driving the plethysmography signal. (**B**) Example of moderate body motion signal (head motion, slow walking) reducing the dominance from the thorax motion on the piezoelectric sensor.

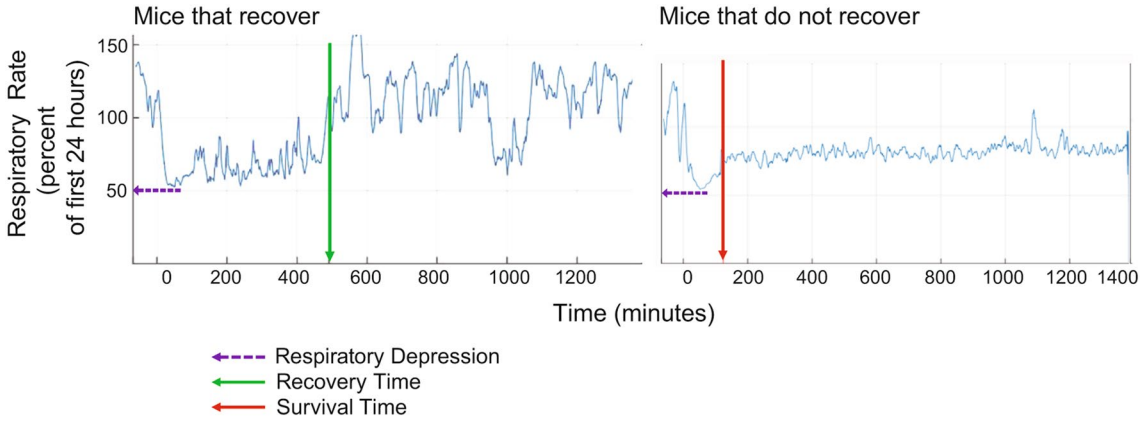

Figure 2. PiezoSleep output for a mouse that recovers and a mouse that fails to recover after opioid treatment. Baseline respiratory rate is first established for 24 h. Time 0, is the time at which morphine is administered. The *blue line* represents the derived respiratory rate trajectories relative to the baseline [defined as the average respiratory rate over the first 24 h (set at 100%)]. Respiratory depression is defined as the lowest percentage of baseline reached after morphine treatment (*purple dotted arrow*). For a mouse that recovers, the *green vertical arrow* indicates recovery time when the respiratory rate returns to baseline. For a mouse that does not recover, the *red vertical arrow* indicates survival time when breathing stops (i.e., piezo output becomes machine noise never returning to baseline).

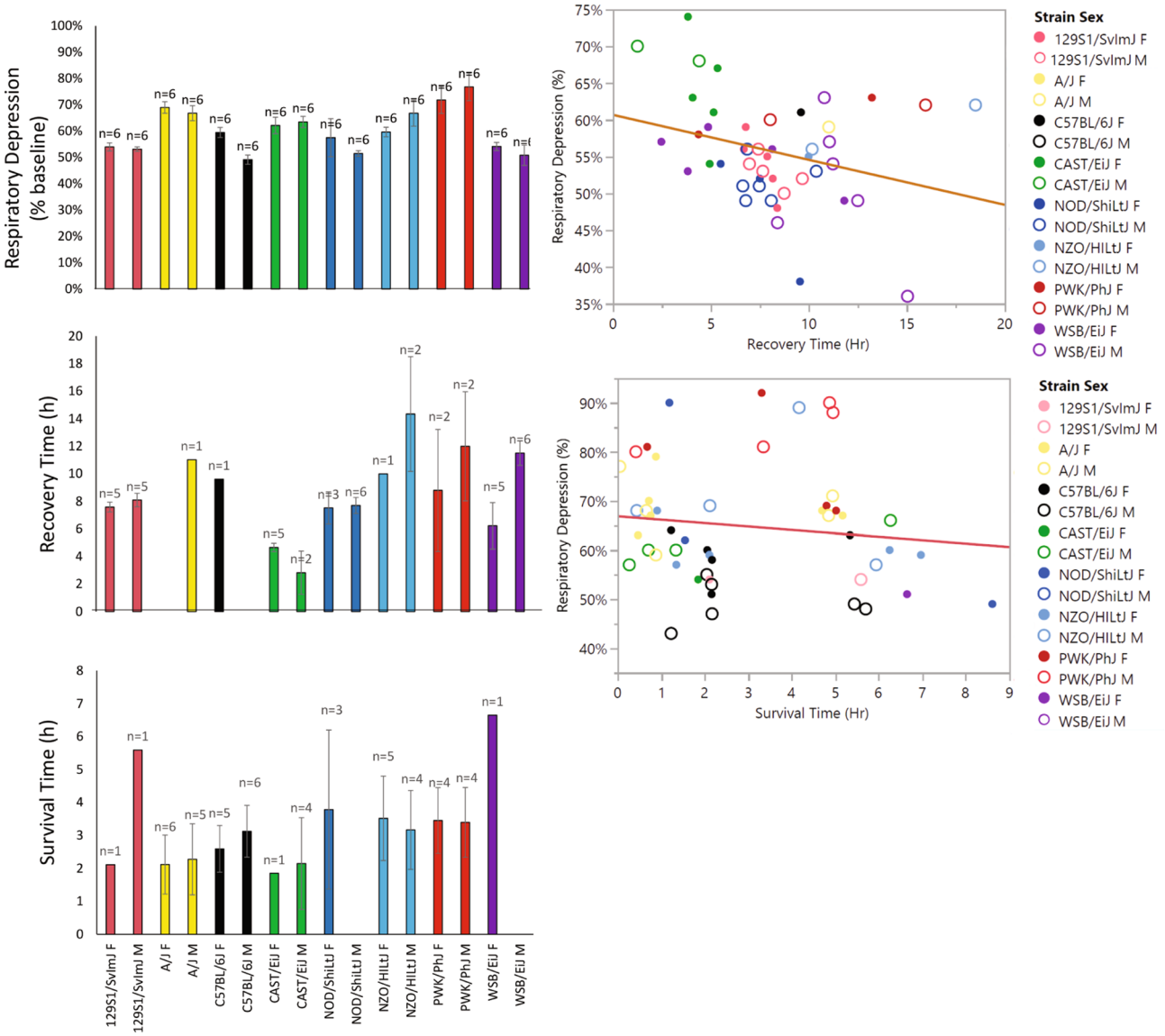

Figure 3. Strain- and sex-specific effect of morphine on respiratory sensitivity. Respiratory depression (top left panel), recovery time (middle left panel) and survival time (bottom left panel) were determined using the probe dose of 436 mg/kg and the PiezoSleep system. The traits of recovery time or survival time are censored such that a mouse does not appear in both graphs as each mouse displays only one of these two phenotypes. Empty bars indicate that no mice fell into this category (i.e., either all recovered, or none recovered). Scatterplot of percent respiratory depression vs recovery time (top right panel) showing a weak correlation of R^2 of 0.08; and a scatterplot of percent respiratory depression vs survival time (bottom right panel) showing no significant correlation. Microsoft 365 https://www.microsoft.com/en-us/microsoft-365?rtc=1 and JMP 15.0.0 https://www.jmp.com.

recovery times (0.05 h to 8.61 h) and survival times that segregate largely by strain, but also by sex (Fig. 3). Respiratory depression at the 436 mg/kg dose showed a significant effect of strain ($F_{strain\ (7,80)} = 10.7357$, $p < 0.0001$), but no sex effect or sex × strain interaction. Using time as the independent variable, we fitted a linear model that revealed significant effects of strain, sex and dose on both recovery time ($F_{(25,152)} = 4.2774$; $p < 0.0001$) and survival time ($F_{(24,162)} = 10.1922$; $p < 0.0001$). These traits are largely uncorrelated. Recovery time and survival time are mutually exclusive traits and each mouse can either recover or fail to recover, not both. We found using a simple linear regression approach that there was a weak correlation [$R^2 = 0.08$, $F_{(1,45)} = 4.1760$, $p = 0.04$] between respiratory depression and recovery time (Fig. 3). The correlation between respiratory depression and survival time was not significant [$R^2 = 0.01$, $F_{(1,49)} = 0.7892$] (Fig. 3). From these quantitative measurements, we calculated the strain intra-class correlation (ICC) as an estimate of heritability and found that respiratory depression ICC = 0.440, recovery time ICC = 0.345 and survival time ICC = 0.338. These values indicate that the traits are heritable and also amenable to genetic mapping. All strain data have been deposited in the Mouse Phenome Database (RRID:SCR_003212 ProjectID:Bubier3).

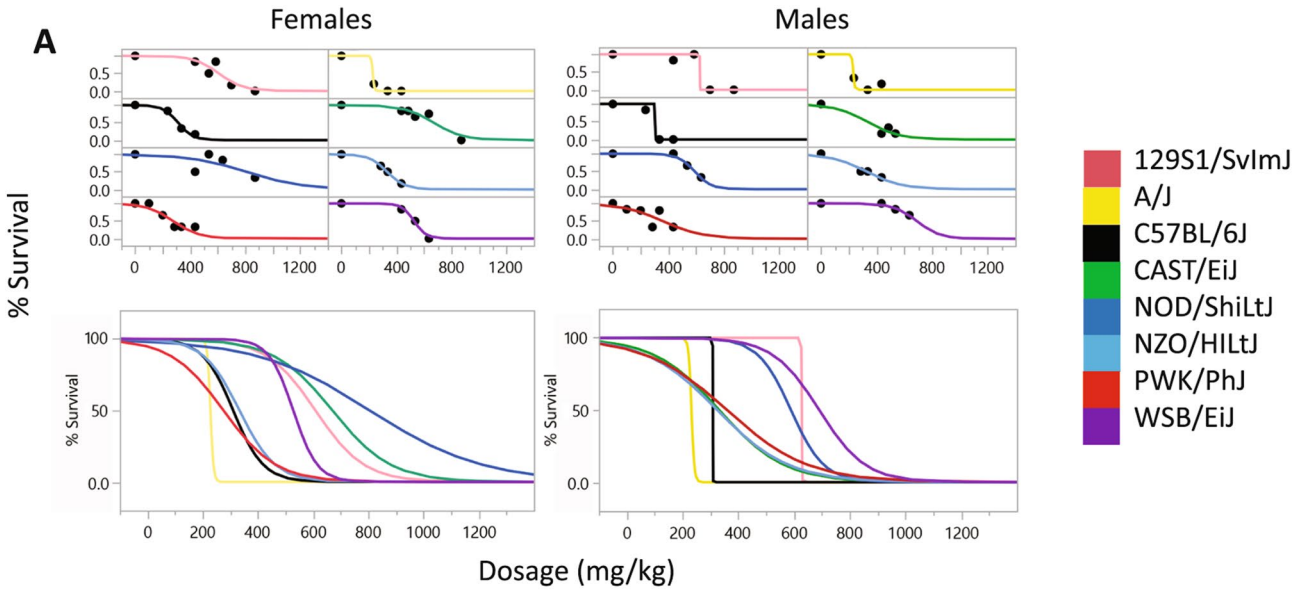

B

Strain and Sex	LD_{50} Morphine (mg/kg)
129S1/SvImJ F	631.3
129S1/SvImJ M	664.2
A/J F	212.2
A/J M	225.2
C57BL/6J F	311.6
C57BL/6J M	254.3
CAST/EiJ F	882.2
CAST/EiJ M	429.9
NOD/ShiLtJ F	811.0
NOD/ShiLtJ M	588.8
NZO/HILtJ F	333.9
NZO/HILtJ M	324.4
PWK/PhJ F	261.0
PWK/PhJ M	359.1
WSB/EiJ F	526.4
WSB/EiJ M	695.6

Figure 4. The morphine LD_{50} by strain and sex. The morphine LD_{50} was determined for each of the eight founder strains and sex using at least six mice in each group and at least three doses of morphine, with at least two doses flanking the LD_{50}. (**A**) Logistic 2-paramater survival curves separated by strain and sex are shown at the top and composites of all strains separated by sex are shown at the bottom. (**B**) The LD_{50} as calculated using the drc package in R and ranged from 212 to 882 mg/kg. JMP 15.0.0 https://www.jmp.com.

LD_{50} determination. Published data reveal a variety of morphine LD_{50} values for mice. In prior studies, using C57BL/6BY and CXB7, the LD_{50} values were 436 mg/kg and 977 mg/kg, respectively[25]. Yoburn et al. have shown that the LD_{50} for different populations of outbred Swiss-Webster mice range from 313 to 745 mg/kg[24]. Based upon this literature, we selected a probe dose of 436 mg/kg. To generate the LD_{50} curve using the minimum number of mice, additional higher or lower doses of morphine were included based on the response to the probe dose until an LD_{50} could be estimated accurately, whereby doses on each side of the 50% mark were tested. Using this approach, survival curves by strain and sex were established (Fig. 4A) and the LD_{50} for each was determined (Fig. 4B). The morphine LD_{50} ranged from 212.2 mg/kg in A/J females to 882.2 mg/kg in CAST/EiJ females. There was not a consistent sex bias up or down across all strains; instead, some LD_{50} values were higher in females than males (e.g., CAST/EiJ and NOD/ShiLtJ), but higher in males than females (e.g., PWK/PhJ and WSB/EiJ).

Genetic mapping in DO mice. To find genetic loci that influence OIRD, quantitative trait loci (QTL) mapping was performed on the respiratory phenotypes using the high diversity, high precision, DO mouse population. A probe dose of 486 mg/kg, chosen based upon the average LD_{50} of the eight founder strains and two sexes, was given to 300 DO mice, 150 of each sex. Of the 300 DO mice entered into the study, 193 (83 females, 110 males) recovered and 107 (67 females, 40 males) did not recover. The quantitative metrics for respiratory

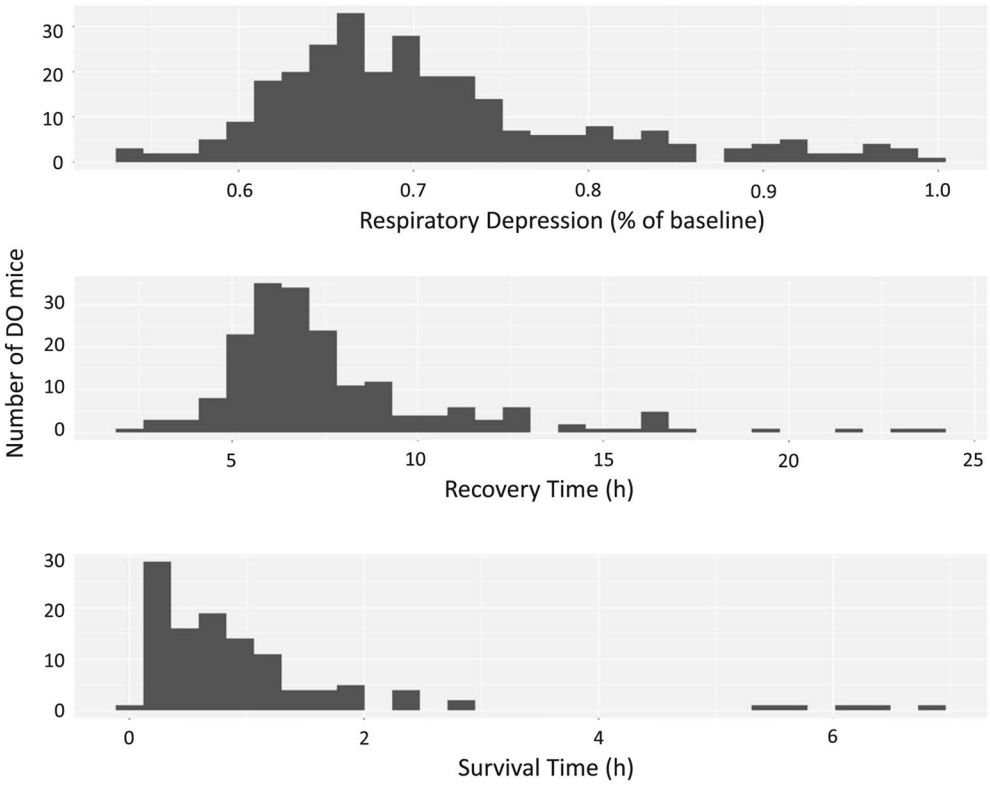

Figure 5. Respiratory response to morphine in Diversity Outbred mice. DO mice were given 486 mg/kg dose of morphine and the respiratory responses were determined by the Piezo Sleep system. The distribution of respiratory responses is shown for respiratory depression (top panel), recovery time (middle panel) and survival time (bottom panel). R/qtl2 https://kbroman.org/qtl2/.

response to morphine, including respiratory depression, recovery time and survival time, all show a continuum of phenotypic diversity (Fig. 5)[31].

Respiratory response QTL. We next mapped QTL in the DO for the three respiratory traits using R/qtl2[30] which implements an eight-state additive haplotype model. A significant QTL was identified for respiratory depression, but no genome-wide significant QTLs were detected for recovery time or survival time using these sample sizes. One suggestive QTL was identified for overall morphine survival using a COXPH model as has previously been used for QTL mapping[32] (Fig. S1).

For the respiratory depression trait, we identified a LOD 9.2 QTL with a 1.5 LOD drop interval on Chr 5:24.30–26.25 (Fig. 6A). The 95% LOD score threshold was 7.65 for $p < 0.05$. The QTL is called *Rdro1* (respiratory depression, response to opioids 1). The *Rdro1* QTL is driven by strong NOD vs. WSB/EiJ allele effects (Fig. 6B). A two-state SNP association analysis identifies potential causative SNPs and results in a reduction of the 1.5 LOD drop credible interval from the peak marker (24.98–26.16 MBp), purple SNPs in Fig. 6C. An ANOVA shows that the peak marker for the respiratory depression phenotype accounts for 42.8% of heritable variation in the DO population.

Identification of candidate genes. Genetic mapping studies are used to identify regions of interest containing variants that influence complex traits. To identify the relevant genes involved in complex trait regulatory mechanisms, there must be evidence of genetic polymorphisms segregating in the population that either influence protein structure or gene expression and evidence of a biological mechanism of action connecting them to the trait, such as expression in a trait-relevant tissue. We identified a 24.98–26.16 MBp credible interval containing 10,782 SNPs (including insertions and deletions) across the DO mice. More specifically using the SNP association mapping model, we found that 1,885 of these SNPs alleles were in the interval (Fig. 6B, Table S1). Of these 1,885 SNPs, eight were in coding regions of genes, 11 were in 5′UTRs, 16 were in 3′UTRs, 861 were intronic, 932 were intergenic, and 107 were in non-coding transcripts (some SNPs have multiple functions, Table S1). Non-coding variants typically influence phenotype through effects on regulation of gene expression via SNPs in regulatory regions, often located in the 5′ UTR, 3′ UTR, introns or within intergenic regulator features. These potential regulatory SNPs are all located in *Speer4a*, *Actr3b*, *Xrcc2*, *Kmt2c*, *Galnt5*, and *Prkag2*. While these SNPs remain candidates for regulation of the respiratory depression phenotype, we focused on coding SNPs because their impact is more readily predictable. The eight coding SNPs lie in four genes (*Galtn11*, *Kmt2c*, *Speer4a*, and *Galnt5*). None of the coding SNPs are the type with the most deleterious effects, such as a stop loss, stop gain

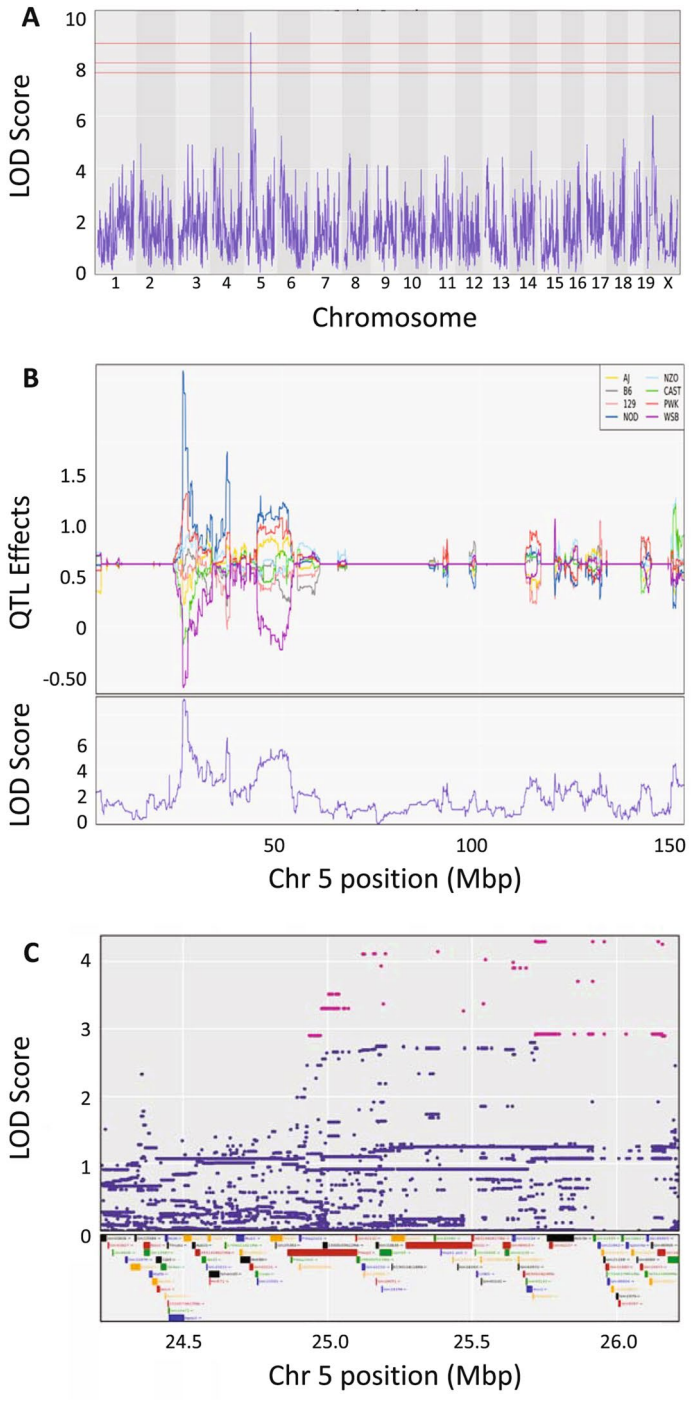

Figure 6. QTL mapping of respiratory depression in DO mice. (**A**) Genome wide scan for QTL regulating the phenotype of respiratory depression in 300 DO mice. (**B**) Allele effect plot of the LOD 9.2 QTL on chromosome 5 for respiratory depression showing a strong narrow peak with LOD confidence interval of 24.98–26.16 MBp. (**C**) A 2MBp interval around the peak locus on chromosome 5 showing the SNPs driving the QTL as well as the genomic features within the interval on chromosome 5. R/qtl2 https://kbroman.org/qtl2/.

or coding region insertion (frameshift). All four of these protein-coding genes are expressed in the mouse pre-Bötzinger complex, a group of brainstem interneurons that control regulation of respiratory rythmogenicity[33], and are thus mechanistically plausible. Three of these four pre-Bötzinger complex-expressed protein-coding genes contain polymorphisms that cause non-synonymous (Cn) amino acid changes. Two of the three changes (serine to threonine at amino acid 702 in *Kmt2c* and asparagine to aspartic acid at amino acid 29 in *Speer4a*) occurred in residues that are not conserved across species. The remaining gene expressed in the pre-Bötzinger

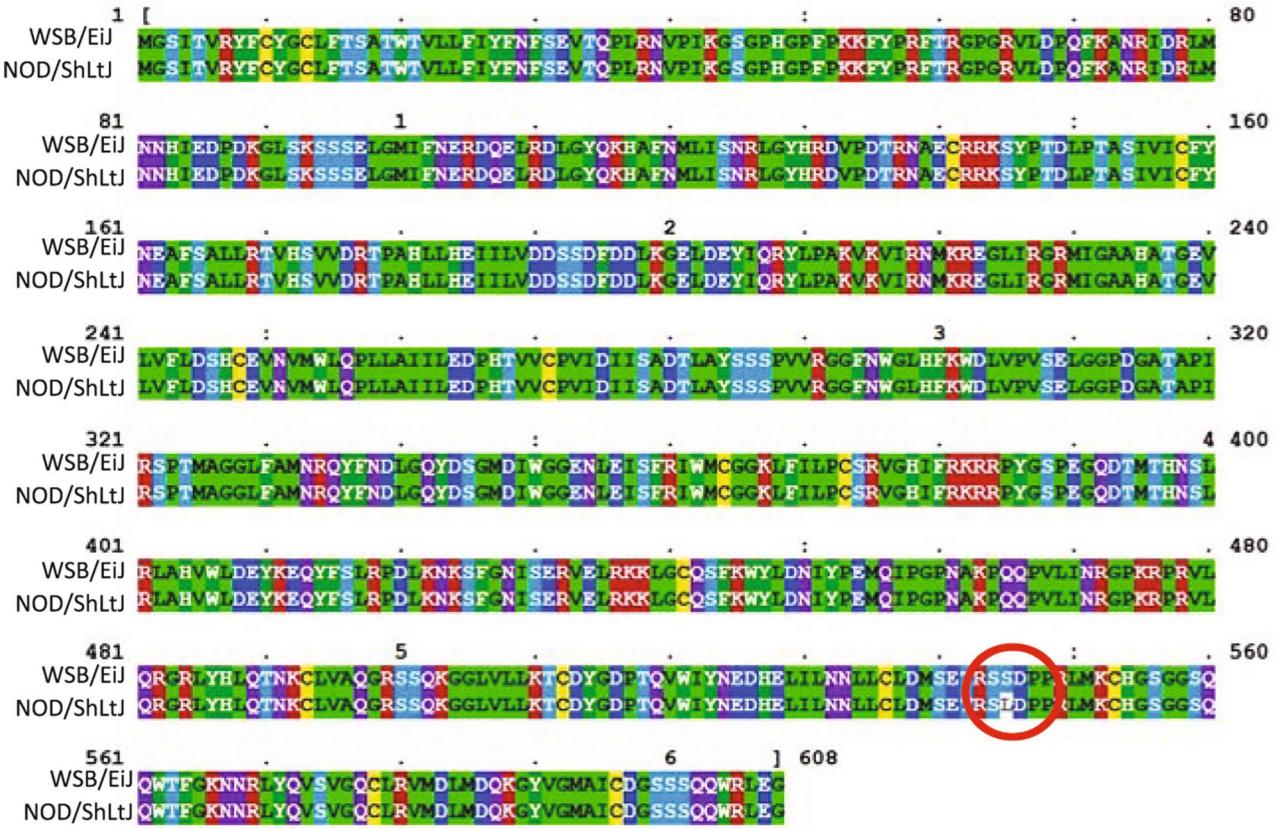

Figure 7. Protein sequence alignment between WSB/EiJ (WSB) and NOD/ShiLtJ (NOD) mice isoforms of GALNT11. The translated GALTNT11 protein sequence encoded by QTL driving alleles WSB and NOD demonstrate sequence homology except for S545L (*red circle*). Yellow = C (capable of disulfide bonding), Green = A, I, L, M, G, P, V (Hydrophobic) Dark Blue = D, E (Negative Charge) , Dark Green = H, W, Y, F (Aromatic/Hydrophobic) Magenta = R, K (Positive Charge) light blue/purple = T, S, Q, N (Polar) Clustal Omega https://www.clustal.org/omega/.

complex and containing a SNP in a conserved coding region is polypeptide *N*-acetylgalactosaminyltransferase 11 (*Galnt11*).

Galnt11 SNP analysis. The *Galnt11* SNP, rs37913166 C/T, changes polar serine residue 545 to a hydrophobic leucine residue (Fig. 7). This amino acid is located within a functional domain that is conserved in vertebrates (Fig. 8A), suggesting that this base change regulates a key functionality. Indeed, this change places the hydrophobic residue, which are generally buried internally, onto the surface of the protein. The 3D protein structure analysis (Fig. 8B) indicates that the non-synonymous serine-to-leucine SNP occurs in a conserved residue within the functional Ricin B lectin domain, a domain generally involved in sugar binding required for glycosylation.

Integrative functional genomic analysis. *GALTN11* is a member of a family of an *N*-acetylgalactosaminyltransferases, which function in O-linked glycosylation. The non-synonymous serine-to-leucine SNP changes a conserved residue within the Ricin B lectin domain of GALNT11 and would be predicted to impede O-linked glycosylation. GALTN11 has been shown to uniquely glycosylate at least 313 glycoproteins in HEK cells[34]. Using the Jaccard similarity tool in the GeneWeaver[35] system for integrative functional genomics, we determined that of the 313 human glycopeptides, 287 mouse orthologs are expressed in the mouse pre-Bötzinger complex[33] (Table S2). Four of those genes *Hs6st2*[36], *Fn1*[37], *Lrp1*[36], and *Sdc4*[38] were identified by the Comparative Toxicogenomic Database[39] as morphine-associated genes, and one additional pre-Bötzinger-expressed glycoprotein, *Cacna2d1*, has been shown to have differential brain expression in mice following morphine treatment[40]. Therefore, variants in *Galnt11* have a plausible mechanism of action through regulation of morphine-associated peptides in the pre-Bötzinger complex.

Discussion

In this study, we found heritable strain differences in the quantitative metrics of respiratory response to morphine, including respiratory depression, recovery time and survival time, using an advanced, high-throughput, behavioral phenotyping protocol. We further identified genomic loci involved in morphine-induced respiratory depression using an unbiased genetic approach. Mapping these traits in the DO mice and evaluation of sequence

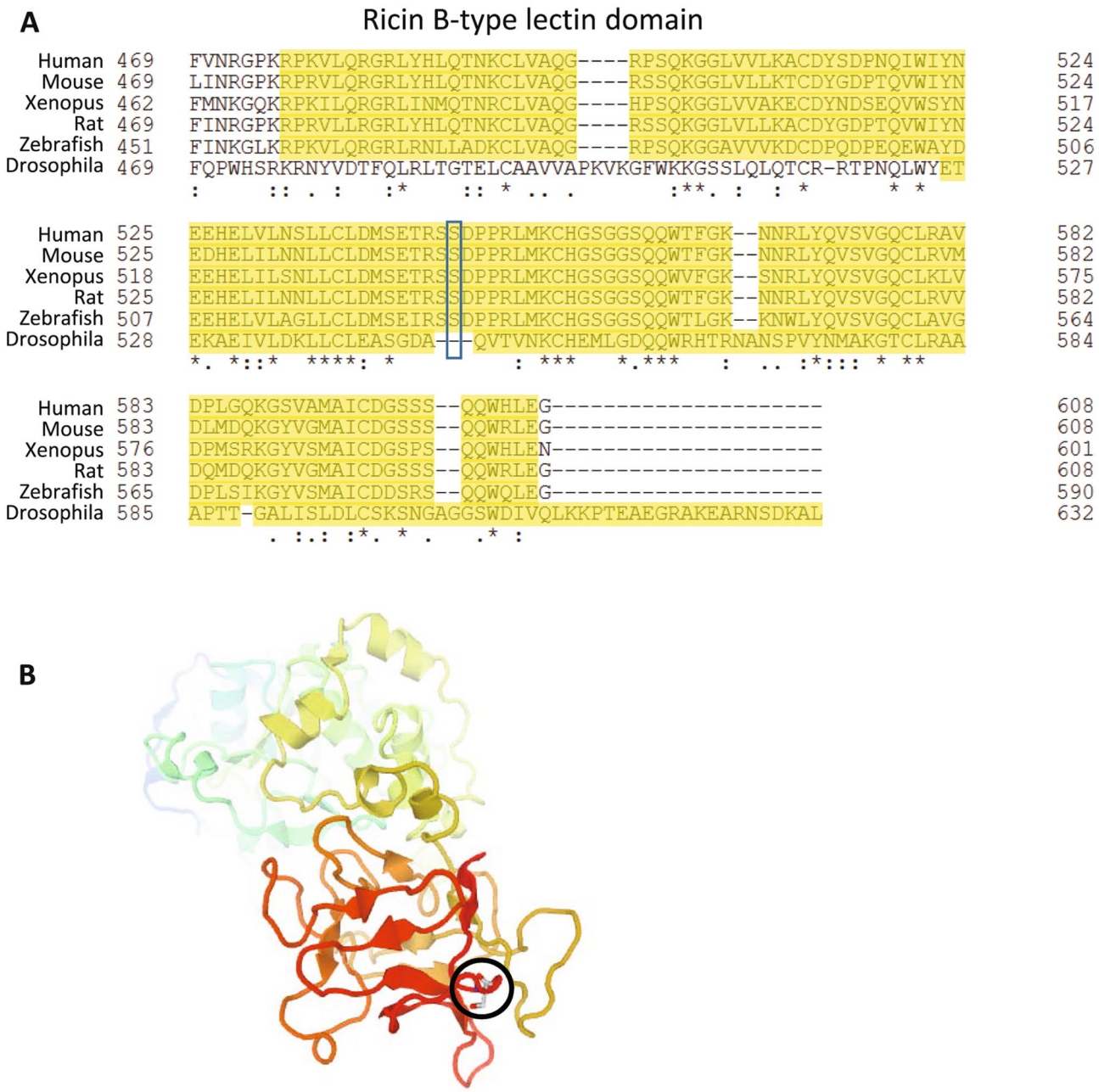

Figure 8. S545L occurs in the Ricin B lectin domain of GALNT11. (**A**) Multi-species alignment of the Ricin B lectin domain of GALNT11 showing that the S545L mutation occurs in a domain conserved across multiple vertebrates, including humans, mice, rats, *Xenopus*, and zebrafish. (**B**) Protein domain map of human GALNT11 showing the localization of the conserved S545L in the Ricin B lectin domain (*black circle*). The 3D structure rendered showing secondary structure as a cartoon type with coloring as a rainbow from N- to C-terminus. Clustal Omega https://www.clustal.org/omega/ Jmol https://jmol.sourceforge.net/.

variants and protein structure, followed by integrative functional genomic analysis in GeneWeaver, has allowed us to implicate *Galnt11* as a candidate gene for respiratory depression in response to morphine.

We identified specific inbred strains of mice that were more sensitive to morphine than other inbred strains of mice. The effect of sex was bidirectional in the inbred CC/DO founder strain population where some males and females differed from each other in either direction depending on strain. The traits of respiratory depression, recovery time and survival time were all shown to have a high degree of heritability. In determining our probe dose for the outbred population, we observed that the LD_{50} for morphine differed by four-fold between these eight parental strains harboring 45 million SNPs, or an equivalent genetic variation as found in the human population.

The traits of respiratory depression, recovery time and survival time were largely independent traits, as seen by their lack of correlation. Strains such as AJ, which had the lowest LD_{50} for both males and females, did not demonstrate the highest degree of respiratory depression, suggesting that factors other than respiratory depression

may play a role in opioid overdose. The lack of correlation between percent respiratory depression and survival time suggest other mechanisms of death in conjunction with OIRD. OIRD results in hypoxia and contributes to cardiac edema[41] a feature found in 96% of fentanyl and 94% of non-fentanyl opioid deaths[42]. Dolinak suggests that other baseline characteristics, such as obstructive sleep apnea, obesity, heart disease and lung disease, make an individual more susceptible to opioid toxicity[43]. Many of the mouse strains involved in this study display these traits naturally, for example NZO/HILt develop severe polygenic obesity[44], C57BL/6 mice show spontaneous apnea and post-sigh apnea[45], and C57BL/6J vs A/J show differences in traits related to cardiac structure and function[46]. The presence of the alleles segregating in the DO population are encouraging for finding additional QTLs related to recovery time and survival time in larger cohorts and possibly using alternatative opioids.

The mechanisms underlying sensitivity to morphine and fentanyl are known to differ in many respects and this same work should be performed for the more potent fentanyl. Morphine is a μ-opioid receptor agonist with significant activities at δ-opioid receptor and κ-opioid receptor subtypes[3,5,47,48], producing potent analgesia. In contrast, fentanyl is a potent (80–100x) high efficacy μ-opioid recepter agonist with much less activity at other opioid receptors[3,5,47,48]. Fentanyl has similarities to morphine with respect to the recruitment of intracellular signaling mechanisms but there are also key differences. For example, fentanyl causes internalization of μ-opioid receptors whereas morphine does not and the development of tolerance to morphine is JNK dependent whereas to fentanyl it is JNK independent. OR events initiated by fentanyl cause greater activation of β-arrestin complexes than do those for morphine[5,20,49–51].

To date, there have been no human GWAS or linkage studies for OIRD. Several GWAS studies have evaluated opioid use disorder (OUD) and/or opioid dependence, and have identified a variety of loci including SNPs linked to OPRM1, KCNG2, CNIH3, LOC647946, LOC101927293, CREB1, PIK3C3, and RGMA[52–57] Additional human linkage studies have identified sex-specific traits[58], epigenetic biomarkers[59] or copy number variations[60] for risk of OUD. Other studies have sought to separate opioid use from opioid dependence, and have thus far identified SNPs associated with SDCCAG8, SLC30A9, and BEND4[61]. Only one study has looked at human opioid overdose risk, specifically by scoring overdose status and determining the number of times that medical treatment was needed in European American populations[54]. In this study, SNPs near MCOLN1, PNPLA6 and DDX18 were identified as overdose risk alleles. Human genes have thus been mapped to opioid use, opioid dependence and opioid overdose susceptibility but human studies are not able to assess opioid-induced respiratory depression, specifically the LD_{50} of an opioid.

Animal studies have allowed us the opportunity to assess the LD_{50} of a drug in a variety of genetic backgrounds and then map those sources of variation. These types of controlled exposure experiments cannot be conducted in humans for which exquisite control of environment is not feasible and prior exposure history is unknown. Our genetic approach of QTL mapping in the DO mouse population has allowed us to identify a genomic region containing no genes previously known to function in opioid pharmacodynamics or pharmacokinetic processes, or implicated in OUD. The genetically diverse structure of this population allows for the identification of narrow genomic intervals often with very few candidate genes. This approach of using advanced mouse populations together with integrative functional genomics has been useful for the prioritization of candidate genes in a variety of different disciplines[62–64].

The identification of *Galnt11* as functioning within the morphine respiratory response reveals a potential new target for therapeutic development. GALNT11 is an *N*-acetylgalactosaminyltransferase that initiates O-linked glycosylation whereby an *N*-acetyl-D-galactosamine residue is transferred to a serine or threonine residue on the target protein. The lectin domain of GALNT11 is the portion that functions to recognize partially glycosylated substrates and direct the glycosylation at nearby sites. This type of post-translational modification controls many phamacokinetic and pharmacodynamic processes as well as the regulation of delta opioid receptor (OPRD1) membrane insertions as O-linked glycosylation is required for proper export of OPRD1 from the ER[65]. O-linked glycosylation is also required for opioid binding peptides, increasing their ability to cross the blood brain barrier[66]. The integrative functional analysis in GeneWeaver identified *Hs6st2*[36], *Fn1*[37], *Lrp1*[36], and *Sdc4*[38] as glycosylation targets of *Galnt11.* All are expressed in the pre-Bötzinger complex and are known to be responsive to morphine further supporting the concept that *Galnt11* is involved in morphine-related responses. Both *Hs6st2* and *Lrp1* were identified as increasing and decreasing, respectively, in responsive to both morphine and stress in C57BL/6J mice[36]. *Fn1* was upregulated six hours post morphine but downregulated four days later[37], and *Sdc4*, a known-μ-μopioid receptor-dependent gene was also upregulated by morphine[38]. The drug-regulated expression of these known glycosylation targets of GALNT11 in relevant tissues further supports the functional relevance of *Galnt11* to OIRD.

Our findings demonstrate the initial mapping of a locus involved in OIRD in mice, for which the likely candidates do not act via the opioid receptor, thereby providing a potential new target for remedial measures. Although it is through mouse genetic variation that we identified this gene, it should be noted that this gene or its glycosylation targets need not vary in humans to be a viable target mechanism for therapeutic discovery and development. Characterization of the role of *Galnt11* and its variants along with other viable candidates will resolve the mechanism further, and continued mapping studies in larger populations will enable detection of additional loci for various aspects of the opioid-induced respiratory response. These findings suggest that phenotypic and genetic variation in the laboratory mouse provides a useful discovery tool for identification of previously unknown biological mechanisms of OIRD.

Methods

Mice. Male (n = 6) and female (n = 6) mice from eight inbred strains including the founders that were used for the DO and CC population [C57BL/6 J, 129S1/SvImJ, A/J, NOD/ShiLtJ, NZO/HlLtJ, /CAST/EiJ, PWK/PhJ, WSB/EiJ] were tested at each dose of morphine. Male and female DO mice (n = 300 including 150 of each sex;

J:DO, JAX stock number 009376) from generation 28 of outcrossing were used. All mice were acquired from The Jackson Laboratory (JAX) and were housed in duplex polycarbonate cages and maintained in a climate-controlled room under a standard 12:12 light–dark cycle (lights on at 0,600 h). Bedding was changed weekly and mice had free access to acidified water throughout the study. Mice were provided free access to food (NIH31 5K52 chow, LabDiet/PMI Nutrition, St. Louis, MO). A Nestlet and Shepherd Shack were provided in each cage for enrichment. Mice were housed in same sex groups of three to five mice per cage. All procedures and protocols were approved by JAX Animal Care and Use Committee and were conducted in compliance with the NIH Guidelines for the Care and Use of Laboratory Animals.

Comparison of piezoelectric sensors and plethysmography for measuring breath rate in mice. A mouse plethysmography chamber was built consisting of a 160 ml plexiglass chamber with ports for air supply and pressure measurement, and end openings outfitted with rubber gaskets to create an airtight seal after closing. A piezo film sensor was sealed into the bottom of the chamber for data collection with PiezoSleep software, with piezo signal sampling set at 120 Hz. Air supply to the chamber occurs through a bias flow regulator supplying air at a constant flow of 300 ml/min, drawn through the chamber via a vacuum. A differential pressure transducer (Biopac) measures the pressure difference between the plethysmography chamber and reference chamber sampled at 200 Hz.

Because the data were recorded on two different systems, an alignment program "BreathCompare", was written to automatically compensate for the difference between subjects internal clocks and to compare breath rates. Signal alignment was done through a simple correlation, which typically indicates time differences of several seconds. The program graphically displays an overlay of the piezo and plethysmography signals for easy visual confirmation. A graphical breath rate overlay allows navigation to intervals of signal disagreement to inspect the signals at these areas.

Morphine. Morphine sulfate pentahydrate (NIDA Drug Supply) was prepared at varying concentrations in sterile saline to deliver doses (200–1,200 mg/kg s.c.) in a manner not to exceed 0.2 ml/10 g body weight. Starting with a dose of 436 mg/kg for all strains and depending upon the result of that dose, the next dose was either increased (536 mg/kg) or decreased (336 mg/kg) for the next cohort, such that doses flanking both sides of the 50% survival point (LD_{50}) were tested. This was repeated with increasing and decreasing doses of 100 mg/kg as necessary depending upon the results of the previous dose. If smaller increments were needed, based upon the results of flanking doses, the dosage was altered by 50 mg/kg or 25 mg/kg. Not all strains received all doses but each strain received at least three doses such that two flanked (one above, one below) the LD_{50}. Using this approach and testing 3–4 doses per strain, the LD_{50} for the eight strains and both sexes was determined and ranged from 212 to 882 mg/kg.

Piezoelectric sleep monitoring to determine respiratory depression, recovery time and survival time. Mice were placed individually into the 7 × 7 inch piezoelectric grid and chamber system (Signal Solutions) for 24 h to equilibrate to the apparatus and collect baseline activity data[27,67]. The mice were housed with approximately ½ cup of pine bedding and ALPHA-dri (Shepard). Individual testing is necessary due to the known enhanced lethality of cage mates during morphine exposure, which has been shown to affect survival[68]. The mice had access to food and water ad libitum while in the chamber. The room was maintained on a 12:12-h light:dark cycle. To control for known circadian effects[69] mice were placed in the chambers between 9 am – 12 pm on Day 1 and were injected with morphine 24 h later. They remained in their chambers undisturbed until 24 h after injection. Whenever possible, complete balanced cohorts of the eight strains and both sexes were run during each of nine replicates of the experiment. The data acquisition computer, food and water were checked daily; otherwise, the mice remained undisturbed. Breath rates were estimated from 4-s intervals in which animal activity dropped low (i.e. during sleep and brief rest periods and pauses during wake), and averaged over 24-min overlapping intervals to provide an average respiratory rate every 12 min. The respiratory rate baseline consisted of the average respiratory rate over the first 24 h, which included both sleep and wake periods. Respiratory rate was then measured in the same way after injection of opioid. These measures were then used to determine thresholds for obtaining the recovery time (respiratory rate returns to baseline, see Fig. 1) or survival time (animal stops moving and breathing, never returning to threshold, see Fig. 1). The 300 DO mice were tested in random cohorts of 36 using the PiezoSleep system with a single 486 mg/kg dose of morphine. This dose was determined as the average LD_{50} dose across the eight strains and two sexes, 16 samples.

Calculating respiratory depression, recovery time and survival time. To test for difference in the respiratory depression, recovery time and survival time across the strains and sexes a linear model was fit, the full model was:

$$\text{Phenotype} = \beta_0\text{Sex} + \beta_1\text{Strain} + \beta_2(\text{Sex} \times \text{Strain}) + \beta_3\text{Dose} + \varepsilon$$

where phenotype was respiratory depression, recovery time or survival time and where ε is random error. The β-parameters were estimated by ordinary least squares, and the type III sum of squares was considered ε in the ANOVA model. In all cases, the full model was fit and reduced by dropping non-significant interactions followed by main effects.

Calculating broad sense heritability (H^2). As a measure of broad sense heritability in the founder strains, the ICC was determined using ICCest from the ICC 2.3.4[70] package in R 4.0.0.

Morphine LD_{50} data analysis. The LD_{50} was calculated using the drc 3.0-1 library[71] in R using the total tested and the observed dead at each dose as a binary or binomial response. A logistic regression model was fit, and a goodness of fit test (based upon Bates and Watts[72]) performed. In addition, a regression model assuming equal LD_{50} across strains was compared by chi square to an LD_{50} assumed different across strains. An adjusted and unadjusted 95% credible interval was also calculated. To graph the data a non-linear 2-parameter model was fit in JMP 14.2.0 (RRID:SCR_014242) with the formula:

$$\frac{1}{\left(1+\mathrm{Exp}(-a\cdot(\mathrm{Dose}-b))\right)}$$

where a = growth rate and b = inflection point.

Genotyping. Tail samples were collected at the conclusion of the experiment and all mice were genotyped using the Giga-MUGA genotyping array (NeoGene). Data were deposited in the DO Database (DODB) RRID:SCR_018180). Genotypes were imputed to a 69 K grid to allow for equal representation across the genome.

QTL mapping. Genotype probabilities were calculated according to the founder genotypes and then converted to allele probabilities. We then interpolated allele probabilities into a grid of 69,000 evenly-spaced genetic intervals[73]. We performed genome scans using R/qtl2 RRID:SCR_018181[31]. Sex and date of test were included as additive covariates. The model includes the random effect of kinship among the DO animals computed using the LOCO method[74]. The significance thresholds were determined for each trait by permutation mapping[75]. The confidence interval around the peak makers was determined using Bayesian support intervals. To determine the percent of variation accounted for by the QTL the mice were classified at the variant into one of eight states based on genotype probabilities of mice at that locus. Following this, a one-way ANOVA was fit to ascertain the strain variation relative to total variation towards estimating heritable variation at that locus. SNP association mapping was also performed using R/qtl2 to test the association of individual SNPs alleles in the region of the locus with the phenotype. Briefly, SNP data were obtained from the SANGER and MGI databases[76,77] for the interval. Using the genotype probabilities and the founder SNP genotypes to infer the SNP genotypes of the DO mice. At each SNP location the eight allele state probabilities are collapsed to two state SNP probabilities and the Cox proportional hazards regression was performed by coxph function in the survival (3.1–12) R package. Based on the output of the log (base e) likelihood for the null model and for the alternative model (with covariates and genotype probabilities), we took the difference of both log likelihoods and then divided by ln(10) to convert the results into the LOD scale. Full QTL mapping scripts are available https://thejacksonlaboratory.github.io/DO_Opioid/index.html.

Candidate gene analysis. In order to assess the plausibility of genes in the QTL interval we identified all SNPs within the additive SNP model segregating between the high and low alleles of the DO founder strains. Next we identified those that were within protein coding region that were most deleterious. Differential coding sequence non-synonymous amino acid substitution SNPs (Cn) that differed between the high and low allele groups were identified. GeneWeaver's database (RRID:SCR_003009) was searched to identify the overlap among tissue-specific expression profiles from Allen Brain Atlas as well as datasets derived from Entrez GEO profiles (RRID:SCR_004584) for pre-Bötzinger neurons[33](GS 273275), diaphragm (GS273269)[78] and lung[79] with the QTL positional candidates. The gene sets were overlapped using the Jaccard similarity and GeneSet graph tools[80].

In order to determine if the Cn SNPS were in areas of evolutionary conservation we aligned the sequence of several species. Representative sequences for each species *Drosophila* (*Q8MVS5*), *Xenopus (Q6DJR8)*, *Danio* (Q08CC3), *Rattus (Q6P6V1)*, *Mus (Q921L8)*, *Homo* (*Q8NCW6*) were acquired from Uniprot (RRID:SCR_002380) and aligned. The Clustal Omega program was used with default parameters[81]. The transition matrix is Gonnet, gap opening penalty of six bits, gap extension of one bit. Clustal-Omega uses the HHalign algorithm and its default settings as its core alignment engine[82]. To determine where the three-dimensional effects of the amino acid change would be we obtained the 3D crystal structure (1XHB)[83] from the Research Collaboratory for Structural Bioinformatics Protein Data Bank (RRID:SCR_012820) and visualized it with Jmol (RRID:SCR_003796)[84].

Integrative functional genomics. In order to assess the functional sufficiency of *Galnt11* as a candidate gene the literature was searched to identify genome-wide studies characterizing glycosylation targets of GALTN11, one study was identified[33] and these genes were added to the GeneWeaver Database (GS356053). Using the Jaccard similarity tool, we overlapped the glycosylation targets with the genes expressed in the mouse pre-Bötzinger complex. We next overlapped these gene with genes identified by the Comparative Toxicogenomic Database (RRID:SCR_006530) as morphine-associated genes.

Data availability

The datasets generated during and/or analysed during the current study are available in the Mouse Phenome Database ProjectID:Bubier3; and in the DO Database (DODB).

Code availability

The R markdown document for the QTL mapping is available at https://thejacksonlaboratory.github.io/DO_Opioid/Plot_DO_morphine.html.

Received: 15 June 2020; Accepted: 11 August 2020
Published online: 11 September 2020

References

1. Boscarino, J. A. *et al.* Risk factors for drug dependence among out-patients on opioid therapy in a large US health-care system. *Addiction* **105**, 1776–1782 (2010).
2. Cicero, T. J., Kasper, Z. A. & Ellis, M. S. Increased use of heroin as an initiating opioid of abuse: Further considerations and policy implications. *Addict. Behav.* **87**, 267–271 (2018).
3. Schmid, C. L. *et al.* Bias factor and therapeutic window correlate to predict safer opioid analgesics. *Cell* **171**, 1165-1175.e13 (2017).
4. Tomassoni, A. J. *et al.* Multiple fentanyl overdoses—New Haven, Connecticut, June 23, 2016. *Morb. Mortal. Wkly. Rep.* **66**, 107–111 (2017).
5. Comer, S. D. & Cahill, C. M. Fentanyl: Receptor pharmacology, abuse potential, and implications for treatment. *Neurosci. Biobehav. Rev.* **106**, 49–57 (2019).
6. May, W. J. *et al.* Morphine has latent deleterious effects on the ventilatory responses to a hypoxic–hypercapnic challenge. *Open J. Mol. Integr. Physiol.* **3**, 134–145 (2013).
7. Pattinson, K. T. Opioids and the control of respiration. *Br. J. Anaesth.* **100**, 747–758 (2008).
8. Frischknecht, H. R., Siegfried, B. & Waser, P. G. Opioids and behavior: Genetic aspects. *Experientia* **44**, 473–481 (1988).
9. Baran, A., Shuster, L., Eleftheriou, B. E. & Bailey, D. W. Opiate receptors in mice: Genetic differences. *Life Sci.* **17**, 633–640 (1975).
10. Shigeta, Y. *et al.* Association of morphine-induced antinociception with variations in the 5′ flanking and 3′ untranslated regions of the mu opioid receptor gene in 10 inbred mouse strains. *Pharmacogenetics Genomics* **18**, 927–936 (2008).
11. Juni, A., Klein, G., Pintar, J. E. & Kest, B. Nociception increases during opioid infusion in opioid receptor triple knock-out mice. *Neuroscience* **147**, 439–444 (2007).
12. Saito, M. *et al.* Variants of kappa-opioid receptor gene and mRNA in alcohol-preferring and alcohol-avoiding mice. *Alcohol* **29**, 39–49 (2003).
13. Kest, B., Hopkins, E., Palmese, C. A., Adler, M. & Mogil, J. S. Genetic variation in morphine analgesic tolerance: A survey of 11 inbred mouse strains. *Pharmacol. Biochem. Behav.* **73**, 821–828 (2002).
14. Wilson, S. G. *et al.* The heritability of antinociception: Common pharmacogenetic mediation of five neurochemically distinct analgesics. *J. Pharmacol. Exp. Therap.* **304**, 547–559 (2003).
15. Smith, S. B. *et al.* Quantitative trait locus and computational mapping identifies Kcnj9 (GIRK3) as a candidate gene affecting analgesia from multiple drug classes. *Pharmacogenetics Genomics* **18**, 231–241 (2008).
16. Kest, B., Palmese, C. A., Juni, A., Chesler, E. J. & Mogil, J. S. Mapping of a quantitative trait locus for morphine withdrawal severity. *Mamm. Genome* **15**, 610–617 (2004).
17. Roerig, S. C. & Fujimoto, J. M. Morphine antinociception in different strains of mice: Relationship of supraspinal–spinal multiplicative interaction to tolerance. *J. Pharmacol. Exp. Therap.* **247**, 603–608 (1988).
18. Belknap, J. K., Noordewier, B. & Lame, M. Genetic dissociation of multiple morphine effects among C57BL/6J, DBA/2J and C3H/HeJ inbred mouse strains. *Physiol. Behav.* **46**, 69–74 (1989).
19. Philip, V. M. *et al.* High-throughput behavioral phenotyping in the expanded panel of BXD recombinant inbred strains. *Genes Brain Behav.* **9**, 129–159 (2010).
20. Bohn, L. M., Gainetdinov, R. R., Lin, F. T., Lefkowitz, R. J. & Caron, M. G. Mu-opioid receptor desensitization by beta-arrestin-2 determines morphine tolerance but not dependence. *Nature* **408**, 720–723 (2000).
21. Belknap, J. K. & Crabbe, J. C. Chromosome mapping of gene loci affecting morphine and amphetamine responses in BXD recombinant inbred mice. *Ann. N. Y. Acad. Sci.* **654**, 311–323 (1992).
22. Fechtner, L., El Ali, M., Sattar, A., Moore, M. & Strohl, K. P. Fentanyl effects on breath generation in C57BL/6J and A/J mouse strains. *Respir. Physiol. Neurobiol.* **215**, 20–29 (2015).
23. Muraki, T. & Kato, R. Strain difference in the effects of morphine on the rectal temperature and respiratory rate in male mice. *Psychopharmacology* **89**, 60–64 (1986).
24. Yoburn, B. C., Kreuscher, S. P., Inturrisi, C. E. & Sierra, V. Opioid receptor upregulation and supersensitivity in mice: Effect of morphine sensitivity. *Pharmacol. Biochem. Behav.* **32**, 727–731 (1989).
25. Moskowitz, A. S., Terman, G. W., Carter, K. R., Morgan, M. J. & Liebeskind, J. C. Analgesic, locomotor and lethal effects of morphine in the mouse: Strain comparisons. *Brain Res.* **361**, 46–51 (1985).
26. Nasser, S. A. & Afify, E. A. Sex differences in pain and opioid mediated antinociception: Modulatory role of gonadal hormones. *Life Sci.* **237**, 116926 (2019).
27. Donohue, K. D., Medonza, D. C., Crane, E. R. & O'Hara, B. F. Assessment of a non-invasive high-throughput classifier for behaviours associated with sleep and wake in mice. *Biomed. Eng. Online* **7**, 14 (2008).
28. Bubier, J. A. *et al.* A microbe associated with sleep revealed by a novel systems genetic analysis of the microbiome in collaborative cross mice. *Genetics* **214**, 719–733 (2020).
29. Philip, V. M. *et al.* Genetic analysis in the collaborative cross breeding population. *Genome Res.* **21**, 1223–1238 (2011).
30. Hou, T. *et al.* Active time-restricted feeding improved sleep-wake cycle in db/db mice. *Front. Neurosci.* **13**, 969 (2019).
31. Broman, K. W. *et al.* R/qtl2: Software for mapping quantitative trait loci with high-dimensional data and multiparent populations. *Genetics* **211**, 495–502 (2019).
32. Durrant, C. *et al.* Collaborative cross mice and their power to map host susceptibility to *Aspergillus fumigatus* infection. *Genome Res.* **21**, 1239–1248 (2011).
33. Hayes, J. A. *et al.* Transcriptome of neonatal preBotzinger complex neurones in Dbx1 reporter mice. *Sci. Rep.* **7**, 8669 (2017).
34. Hintze, J. *et al.* Probing the contribution of individual polypeptide GalNAc-transferase isoforms to the O-glycoproteome by inducible expression in isogenic cell lines. *J. Biol. Chem.* **293**, 19064–19077 (2018).
35. Baker, E., Bubier, J. A., Reynolds, T., Langston, M. A. & Chesler, E. J. GeneWeaver: Data driven alignment of cross-species genomics in biology and disease. *Nucl. Acids Res.* **44**, D555–D559 (2015).
36. Juul, S. E., Beyer, R. P., Bammler, T. K., Farin, F. M. & Gleason, C. A. Effects of neonatal stress and morphine on murine hippocampal gene expression. *Pediatr. Res.* **69**, 285–292 (2011).
37. Anghel, A. *et al.* Gene expression profiling following short-term and long-term morphine exposure in mice uncovers genes involved in food intake. *Neuroscience* **167**, 554–566 (2010).
38. Le Merrer, J. *et al.* Protracted abstinence from distinct drugs of abuse shows regulation of a common gene network. *Addict. Biol.* **17**, 1–12 (2012).
39. Davis, A. P. *et al.* The comparative toxicogenomics database: Update 2013. *Nucl. Acids Res.* **41**, D1104–D1114 (2013).
40. Shibasaki, M., Katsura, M., Kurokawa, K., Torigoe, F. & Ohkuma, S. Regional differences of L-type high voltage-gated calcium channel subunit expression in the mouse brain after chronic morphine treatment. *J. Pharmacol. Sci.* **105**, 177–183 (2007).
41. White, J. M. & Irvine, R. J. Mechanisms of fatal opioid overdose. *Addiction* **94**, 961–972 (1999).
42. Pelletier, D. E. & Andrew, T. A. Common findings and predictive measures of opioid overdoses. *Acad. Forensic Pathol.* **7**, 91–98 (2017).
43. Dolinak, D. Opioid toxicity. *Acad. Forensic Pathol.* **7**, 19–35 (2017).

44. Bielschowsky, M. A new strain of mice with hereditary obesity. *Proc. Univ. Otago Med. Sch.* **31**, 29–31 (1953).
45. Yamauchi, M., Kimura, H. & Strohl, K. P. Mouse models of apnea: Strain differences in apnea expression and its pharmacologic and genetic modification. *Adv. Exp. Med. Biol.* **669**, 303–307 (2010).
46. Hoit, B. D. *et al.* Naturally occurring variation in cardiovascular traits among inbred mouse strains. *Genomics* **79**, 679–685 (2002).
47. Morgan, M. M. & Christie, M. J. Analysis of opioid efficacy, tolerance, addiction and dependence from cell culture to human. *Br. J. Pharmacol.* **164**, 1322–1334 (2011).
48. Williams, J. T. *et al.* Regulation of μ-opioid receptors: Desensitization, phosphorylation, internalization, and tolerance. *Pharmacol. Rev.* **65**, 223–254 (2013).
49. Bohn, L. M. *et al.* Enhanced morphine analgesia in mice lacking beta-arrestin 2. *Science* **286**, 2495–2498 (1999).
50. Ligeza, A., Wawrzczak-Bargiela, A., Kaminska, D., Korostynski, M. & Przewlocki, R. Regulation of ERK1/2 phosphorylation by acute and chronic morphine—Implications for the role of cAMP-responsive element binding factor (CREB)-dependent and Ets-like protein-1 (Elk-1)-dependent transcription; small interfering RNA-based strategy. *FEBS J.* **275**, 3836–3849 (2008).
51. Raehal, K. M. & Bohn, L. M. The role of beta-arrestin2 in the severity of antinociceptive tolerance and physical dependence induced by different opioid pain therapeutics. *Neuropharmacology* **60**, 58–65 (2011).
52. Gelernter, J. *et al.* Genome-wide association study of opioid dependence: Multiple associations mapped to calcium and potassium pathways. *Biol. Psychiatry* **76**, 66–74 (2014).
53. Brick, L. A., Micalizzi, L., Knopik, V. S. & Palmer, R. H. C. Characterization of DSM-IV opioid dependence among individuals of European ancestry. *J. Stud. Alcohol Drugs* **80**, 319–330 (2019).
54. Cheng, Z. *et al.* Genome-wide association study identifies a regulatory variant of RGMA associated with opioid dependence in European Americans. *Biol. Psychiatry* **84**, 762–770 (2018).
55. Smith, A. H. *et al.* Genome-wide association study of therapeutic opioid dosing identifies a novel locus upstream of OPRM1. *Mol. Psychiatry* **22**, 346–352 (2017).
56. Nelson, E. C. *et al.* Evidence of CNIH3 involvement in opioid dependence. *Mol Psychiatry* **21**, 608–614 (2016).
57. Nishizawa, D. *et al.* Genome-wide association study identifies a potent locus associated with human opioid sensitivity. *Mol. Psychiatry* **19**, 55–62 (2014).
58. Yang, B. Z., Han, S., Kranzler, H. R., Palmer, A. A. & Gelernter, J. Sex-specific linkage scans in opioid dependence. *Am. J. Med. Genet. B Neuropsychiatr. Genet.* **174**, 261–268 (2017).
59. Montalvo-Ortiz, J. L., Cheng, Z., Kranzler, H. R., Zhang, H. & Gelernter, J. genomewide study of epigenetic biomarkers of opioid dependence in European–American women. *Sci. Rep.* **9**, 4660 (2019).
60. Li, D. *et al.* Genome-wide association study of copy number variations (CNVs) with opioid dependence. *Neuropsychopharmacology* **40**, 1016–1026 (2015).
61. Polimanti, R. *et al.* Leveraging genome-wide data to investigate differences between opioid use vs. opioid dependence in 41,176 individuals from the Psychiatric Genomics Consortium. *Mol. Psychiatry* https://doi.org/10.1038/s41380-020-0677-9 (2020).
62. Delprato, A. *et al.* QTL and systems genetics analysis of mouse grooming and behavioral responses to novelty in an open field. *Genes Brain Behav.* **16**, 790–799 (2017).
63. Recla, J. M. *et al.* Genetic mapping in diversity outbred mice identifies a Trpa1 variant influencing late-phase formalin response. *Pain* **160**, 1740–1753 (2019).
64. Recla, J. M. *et al.* Precise genetic mapping and integrative bioinformatics in diversity outbred mice reveals Hydin as a novel pain gene. *Mamm. Genome* **25**, 211–222 (2014).
65. Petaja-Repo, U. E., Hogue, M., Laperriere, A., Walker, P. & Bouvier, M. Export from the endoplasmic reticulum represents the limiting step in the maturation and cell surface expression of the human delta opioid receptor. *J. Biol. Chem.* **275**, 13727–13736 (2000).
66. Egleton, R. D. *et al.* Improved blood–brain barrier penetration and enhanced analgesia of an opioid peptide by glycosylation. *J. Pharmacol. Exp. Therap.* **299**, 967–972 (2001).
67. Flores, A. E. *et al.* Pattern recognition of sleep in rodents using piezoelectric signals generated by gross body movements. *IEEE Trans. Bio-Med. Eng.* **54**, 225–233 (2007).
68. Mohrland, J. S. & Craigmill, A. L. Possible mechanism for the enhanced lethality of morphine in aggregated mice. *Pharmacol. Biochem. Behav.* **13**, 475–477 (1980).
69. Campos, A. E., Lujan, M., Lopez, E., Figueroa-Hernandez, J. L. & Rodriguez, R. Circadian variation in the lethal effect of morphine in the mouse. *Proc. West. Pharmacol. Soc.* **26**, 101–103 (1983).
70. Wolak, W. M. ICC. https://doi.org/10.5281/zenodo.1471655 (2016).
71. Ritz, M. C., Lamb, R. J., Goldberg, S. R. & Kuhar, M. J. Cocaine receptors on dopamine transporters are related to self-administration of cocaine. *Science* **237**, 1219–1223 (1987).
72. Bates, D. M. & Watts, D. G. *Nonlinear Regression Analysis and Its Applications* (Wiley, London, 1988).
73. Chick, J. M. *et al.* Defining the consequences of genetic variation on a proteome-wide scale. *Nature* **534**, 500–505 (2016).
74. Yang, J., Zaitlen, N. A., Goddard, M. E., Visscher, P. M. & Price, A. L. Advantages and pitfalls in the application of mixed-model association methods. *Nat. Genet.* **46**, 100–106 (2014).
75. Sen, S. & Churchill, G. A. A statistical framework for quantitative trait mapping. *Genetics* **159**, 371–387 (2001).
76. Yalcin, B. *et al.* Sequence-based characterization of structural variation in the mouse genome. *Nature* **477**, 326–329 (2011).
77. Bult, C. J. *et al.* Mouse genome database (MGD) 2019. *Nucl. Acids Res.* **47**, D801–D806 (2019).
78. van Lunteren, E., Moyer, M. & Leahy, P. Gene expression profiling of diaphragm muscle in alpha2-laminin (merosin)-deficient dy/dy dystrophic mice. *Physiol. Genomics* **25**, 85–95 (2006).
79. Steed, A. L. *et al.* The microbial metabolite desaminotyrosine protects from influenza through type I interferon. *Science* **357**, 498–502 (2017).
80. Baker, E., Bubier, J. A., Reynolds, T., Langston, M. A. & Chesler, E. J. GeneWeaver: Data driven alignment of cross-species genomics in biology and disease. *Nucleic Acids Res.* **44**, D555–D559 (2016).
81. Sievers, F. *et al.* Fast, scalable generation of high-quality protein multiple sequence alignments using clustal omega. *Mol. Syst. Biol.* **7**, 539 (2011).
82. Soding, J. Protein homology detection by HMM–HMM comparison. *Bioinformatics* **21**, 951–960 (2005).
83. Fritz, T. A., Hurley, J. H., Trinh, L. B., Shiloach, J. & Tabak, L. A. The beginnings of mucin biosynthesis: The crystal structure of UDP-GalNAc:Polypeptide alpha-N-acetylgalactosaminyltransferase-T1. *Proc. Natl. Acad. Sci. USA* **101**, 15307–15312 (2004).
84. Jmol Development Team. Jmol: An open-source Java viewer for chemical structures in 3D. (2001).

Acknowledgements

Funding R01 DA037927, R01 AA018776 and P50 DA039841to EJC, R01 DA048890 to JAB, R41 HL142489-01 to RB, KFD and BFO and the NIDA Drug Supply Program. Special thanks to Jennifer Ryan and the Center for Biometric analysis at JAX for use of the PiezoSleep system and to Stephen Krasinski for extensive edits of the manuscript.

Author contributions

J.A.B., K.D.D., B.F.O, EJC Conception or design of the work J.A.B., T.R, C.M.H R.B. Data collection. J.A.B., H.H, V.M.P, R.B. K.D.D., B.F.O Data analysis and interpretation J.A.B., E.J.C. R.B., K.D.D, B.F.O Drafting and revising the article J.A.B., H.H., V.M.P., T.R., C.M.H, R.B. K.D.D, K.F.O, E.J.C. Final approval of the version to be published.

Competing interests

B.F.O. and K.D.D. are co-founders and co-owners of Signal Solutions that manufactures and sells the Piezoelectric technology utilized in this study.

Additional information

Supplementary information is available for this paper at https://doi.org/10.1038/s41598-020-71804-2.

Correspondence and requests for materials should be addressed to J.A.B.

Reprints and permissions information is available at www.nature.com/reprints.

Publisher's note Springer Nature remains neutral with regard to jurisdictional claims in published maps and institutional affiliations.